

Anomalous transport and chaotic advection in homogeneous porous media

D. R. Lester*

Mathematics, Informatics and Statistics, CSIRO, PO Box 56, Highett, Victoria 3190, Australia and School of Civil, Environmental and Chemical Engineering, Royal Melbourne Institute of Technology, Melbourne, Victoria 3001, Australia

G. Metcalfe

Materials Science and Engineering, CSIRO, PO Box 56, Highett, Victoria 3190, Australia

M. G. Trefry

Land and Water, CSIRO, Private Bag 5, Wembley, Western Australia 6913, Australia and School of Earth and Environment, The University of Western Australia, 35 Stirling Highway, Crawley, Western Australia 6009, Australia

(Received 10 August 2014; published 19 December 2014)

The topological complexity inherent to all porous media imparts persistent chaotic advection under steady flow conditions, which, in concert with the no-slip boundary condition, generates anomalous transport. We explore the impact of this mechanism upon longitudinal dispersion via a model random porous network and develop a continuous-time random walk that predicts both preasymptotic and asymptotic transport. In the absence of diffusion, the ergodicity of chaotic fluid orbits acts to suppress longitudinal dispersion from ballistic to superdiffusive transport, with asymptotic variance scaling as $\sigma_L^2(t) \sim t^2/(\ln t)^3$. These results demonstrate that anomalous transport is inherent to homogeneous porous media and has significant implications for macrodispersion.

DOI: [10.1103/PhysRevE.90.063012](https://doi.org/10.1103/PhysRevE.90.063012)

PACS number(s): 47.51.+a, 05.45.-a, 47.52.+j

Porous media flows host a vast range of natural and synthetic processes: From the earth's crust, which contains most of civilization's energy and mineral and water reserves, to biological tissue, such as cartilage and vascular networks, fluids are continually transporting, mixing, and reacting species through porous structures. As the detailed flow structure and Lagrangian dynamics significantly impact fluid-borne processes [1–5], understanding the key physical mechanisms that control transport and dispersion in porous media is a problem of widespread concern.

Transport in porous media is a truly multiscale process, ranging from Stokes flow at the pore scale to macroscopic Darcy flow, which may be highly heterogeneous. This complexity lies at the root of the long-standing problem of developing macroscopic closures and scaling laws for transport in heterogeneous media, which is typically observed to be anomalous or non-Fickian [4,6,7], such that the mean-square displacement grows nonlinearly in time [8]. Modeling approaches typically link pore-scale and Darcy-scale dispersion by consideration of transport at a locally homogeneous support scale ω [9], where transport is commonly assumed to be Fickian.

Hence the question of whether non-Fickian transport can occur within *homogeneous* media is of paramount importance to studies of transport, with important implications for the prediction of, e.g., transport of groundwater pollutants [10] and geothermal energy [11]. There exists some controversy as to the validity of the assumption of Fickian transport in homogeneous media, and several experimental [12–15] and numerical [16–18] investigations observe persistent non-

Fickian transport at the support scale ω . This behavior is often attributed to so-called hold-up dispersion arising from dead-end pores and/or recirculation zones. Several theoretical studies [9,19] argue that in the absence of these features pore-scale transport is Fickian due to the analogy with Taylor-Aris dispersion [20,21] for a set of pores connected in series.

Recently it was established [22] that an alternate mechanism by which anomalous transport may occur in homogeneous porous media is via chaotic advection at the pore scale. As chaotic advection is well known to impart anomalous transport for passive tracer particles [23,24] in boundary-dominated flows, the ubiquitous nature of this mechanism means that anomalous transport is possible in all homogeneous porous media. In this paper we show that anomalous transport is inherent to all three-dimensional (3D) random porous media due to interactions between fluid stretching at stagnation points and the no-slip boundary condition.

To quantify this phenomenon we consider transport in an ideal 3D random network that contains the minimum topological complexity and disorder common to all homogeneous porous media. While real homogeneous media are more complex, we show such additional complexity still generates chaotic advection and anomalous transport. We perform numerical simulations of transport in this ideal network and develop a continuous-time random walk (CTRW) framework to describe transport and derive expressions for preasymptotic and asymptotic longitudinal dispersion. As these underlying mechanisms are common to all porous media, whether homogeneous or heterogeneous at large scales, they have significant implications for upscaling of porous media transport models and generate significant insights into the nature of transport in porous media.

The topological complexity inherent to all porous media generates a large number density of nondegenerate equilibrium

*daniel.lester@rmit.edu.au

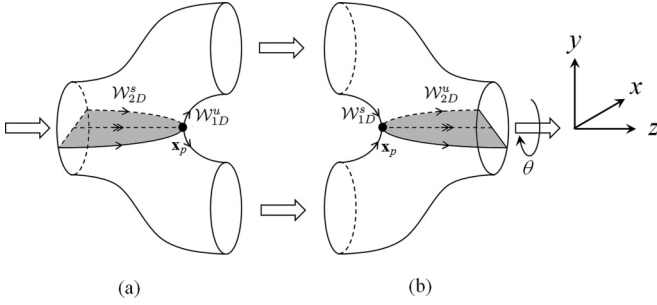


FIG. 1. Schematic of (a) pore branch element Ω and (b) pore merger element, with the nondegenerate equilibrium stagnation (reentrant) point shown and the associated 2D unstable (stable) manifold, representing the skeleton of flow comprised of surfaces of a locally minimum flux. Note that for the angle $\theta \neq 0$ the minimal flux surfaces are transversely oriented.

(stagnation) points \mathbf{x}_p under steady 3D flow [22], as shown in Fig. 1 for the case of an open porous network. Due to continuity, these stagnation points impart a series of punctuated local stretching and folding events (the hallmark of chaotic dynamics in continuous systems) as the fluid continuum is advected through the network. These stagnation points are predominantly of saddle type (due to the Poincaré-Hopf theorem and strongly negative Euler characteristic typical of porous media [25,26]) and so the associated unstable \mathcal{W}_{2D}^U (stable \mathcal{W}_{2D}^S) manifolds that project into the fluid bulk are co-dimension 1 (two dimensional) and form the “skeleton of the flow” [27] that organizes transport and mixing. In concert with folding of material elements due to downstream advection, fluid stretching at these stagnation points imparts ubiquitous and persistent chaotic advection in all topologically complex media under steady flow conditions [22].

Chaotic Lagrangian dynamics are well known to significantly alter transport dynamics in flow systems, exemplified by the impact of transverse chaotic advection upon boundary-dominated flows [23,24], where the ergodicity of fluid particle trajectories acts to suppress longitudinal dispersion. In the absence of diffusion, transverse chaotic advection acts to retard the evolution of longitudinal variance $\sigma_L^2(t)$ [related to longitudinal dispersion as $D_L(t) = \sigma_L^2(t)/2t$] from ballistic scaling [$\sigma_L^2(t) \sim t^2$] due to the no-slip boundary condition to superdiffusive transport [$\sigma_L^2(t) \sim t^\alpha$, $1 < \alpha < 2$]. While analogous to Taylor-Aris dispersion under molecular diffusion, this mechanism is distinctly different in that chaotic advection is hydrodynamic (geometric) in origin and deterministic and so cannot be modeled via a simple Fickian diffusion process [23,24].

Although a formal link is yet to be established [28], chaotic dynamics and ergodicity are strongly associated with decaying correlations along Lagrangian trajectories [29]; it is this mechanism that suppresses longitudinal dispersion in boundary-dominated flows. Due to such ergodicity and the punctuated nature of stretching events at stagnation points, fluid transport and deformation in porous media flows may be described as a stochastic process (where the validity of this approximation is quantified by the infinite-time Lyapunov exponent λ_∞).

We formalize this stochastic process in terms of a CTRW, whereby the displacements $\Delta \mathbf{x}$ and transition times Δt between stagnation points arise respectively from the pore-scale geometry and advection field. If we consider the evolution of a fluid particle propagating in the mean flow direction z , then in the absence of diffusion the spatial position $\mathbf{x} = \{x, y, z\}$ and residence time t of the fluid particle evolve via the CTRW

$$t_{n+1} = t_n + \Delta t_n, \quad (1)$$

$$\mathbf{x}_{n+1} = \mathbf{x}_n + \Delta \mathbf{x}_n, \quad (2)$$

where the temporal and spatial increments are distributed via the probability distribution functions (PDFs) $\psi(\Delta t)$ and $\rho_{\Delta \mathbf{x}}(\Delta \mathbf{x})$, respectively.

To directly study the impact of chaotic advection upon transport, we consider an ideal 3D open porous network model (see [30] for details) based upon a series of randomly connected (and oriented) alternating pore branches and mergers shown in Fig. 1. This idealized network represents the minimum topological complexity and disorder common to all random porous media and exhibits chaotic advection and anomalous transport as a result of these features. While real homogeneous media contain additional features such as distributions of pore diameter, surface roughness, pore curvature, and tortuosity, as well as greater topological complexity that augments transport phenomena, chaotic advection arising from topological complexity persists in the presence of such features (indeed, features such as surface roughness [31] and pore curvature [24] also generate chaotic advection). Hence the qualitative features of the results herein are universal to all porous media and we also explore the quantitative impact of deviations from ideality upon asymptotic transport. We compare longitudinal dispersion predicted by this ideal model network to a stochastic stretching CTRW based upon the network kernels ψ and $\rho_{\Delta \mathbf{x}}$. One criticism of CTRW models is that it can be difficult to relate the increment kernels to physical processes; in this case ψ and $\rho_{\Delta \mathbf{x}}$ are directly quantified in terms of fluid deformation and advection, providing a clear link with the pore-scale microstructure. Numerical calculations [30] of 3D Stokes flow through the pore branch (merge) element in Fig. 1(a) [Fig. 1(b)] shows that advection is remarkably well approximated (within error $\epsilon \sim 10^{-3}$) by the analytic spatial \mathcal{M} (\mathcal{M}^{-1}) and temporal \mathcal{T} maps

$$\mathcal{M}: \{x_r, y_r\} \mapsto \{x_r, 2y_r - |y_r|/y_r \sqrt{1 - x_r^2}\}, \quad (3)$$

$$\mathcal{T}: t \mapsto t + \frac{1}{1 - x_r^2 - y_r^2}, \quad (4)$$

where $\{x_r, y_r\}$ are the scaled x and y particle positions relative to the pore boundary at the inlet and outlet such that $x_r^2 + y_r^2 = 0(1)$ corresponds to the pore center (boundary). Remarkably, the no-slip boundary condition in Ω generates a residence time distribution (4) very similar to that of a Poiseuille flow such that the residence time in the pore branch and merger is quantified by the composite operators $\mathcal{T} \circ \mathcal{M}$ and $\mathcal{T} \circ \mathcal{M}^{-1}$, respectively.

Although zero-net-fluid deformation occurs over the coupled pore branch and merger (couplet) shown in Fig. 1 (as

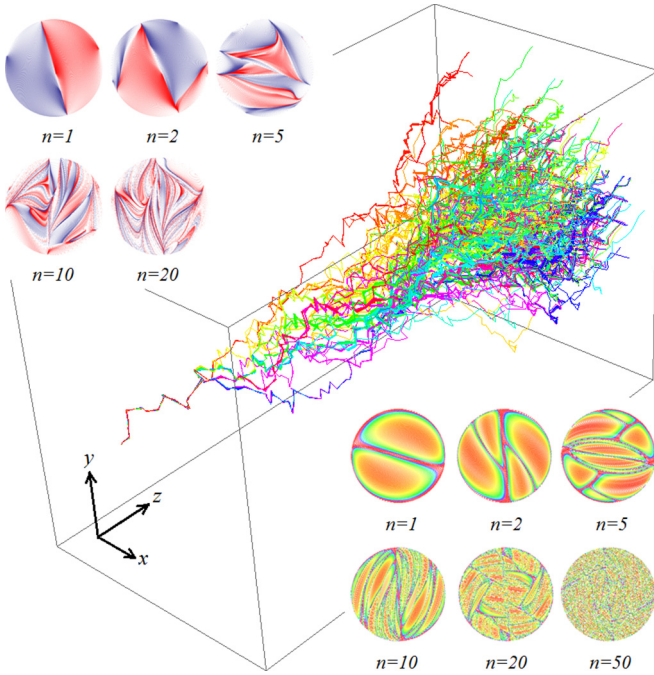


FIG. 2. (Color online) Evolution of pointwise tracer injection in the dimensionless 3D network model (center) with dye trace (top left) and a residence time distribution (RTD) (bottom right), ranging from maximum residence time [black (red)] to the minimum time [white (orange)] evolution shown as the number n of pore branches or mergers. Ergodic mixing of black and gray (red and blue) particles within a pore (top left) leads to redistribution of the RTD (bottom right), suppressing longitudinal variance.

$\mathcal{M}^{-1} \circ \mathcal{M} = I$, where I is the identity operator), random orientation in the xy plane of these elements (as quantified by θ) breaks this symmetry, where the reoriented maps

$$S(\theta) := R(\theta) \circ \mathcal{M} \circ R(-\theta), \quad (5)$$

$$S^{-1}(\theta) := R(\theta) \circ \mathcal{M}^{-1} \circ R(-\theta) \quad (6)$$

yield $S(\theta_1) \circ S(\theta_2) \neq I$ in general. These maps (4)–(6) quantify fluid transport and deformation over a pore branch or merger and so when appropriately concatenated, they model transport over a given realization of the 3D random network (where θ is uniformly distributed; see [30] for details) and recover the transverse stretching infinite-time Lyapunov exponent $\lambda_\infty \approx 0.11780$ derived in [22]. This model captures both macroscopic dispersion [as shown by the evolution of a point source of 10^5 fluid particles in a given realization of the network in Fig. 2 (center)] and pore-scale dispersion, where chaotic mixing arises (Fig. 2, upper left) that is similar to that in 3D static mixers [32,33]. Such transverse mixing generates nontrivial residence time distributions (Fig. 2, lower right), which suppress longitudinal dispersion arising from the no-slip boundary condition.

To develop a CTRW formulation of transport in the 3D pore network model, we consider the residence time increment kernel $\psi(\Delta t)$ as a stochastic process based upon the temporal map \mathcal{T} (4), which generates a power-law distribution of travel

times

$$\psi(\Delta t) = \begin{cases} \Delta t^{-2}, & \Delta t \geq 1 \\ 0, & \Delta t < 1, \end{cases} \quad (7)$$

where all nonzero moments of $\psi(\Delta t)$ are unbounded due to the power-law tail arising from the no-slip boundary condition. Such distributions are known to generate non-Fickian or anomalous transport [34]. To provide general results, the spatial increment kernel $\rho_{\Delta \mathbf{x}}$ is unspecified, except that it is bounded with finite variance.

To investigate longitudinal dispersion in the 3D porous network, we first use the CTRW model to calculate the PDF $P(\mathbf{x}, t)$ of an ensemble of particles moving through the random network. From a formal ensemble average [35], the generalized master equation (GME) provides a quantitative solution of $P(\mathbf{x}, t)$ from the CTRW (2) and (1). A second-order moment expansion of the Laplace transform of the GME yields a Fokker-Planck equation for the PDF $\bar{P}(\mathbf{x}, u)$ [36] in Laplace time u as

$$u \bar{P}(\mathbf{x}, u) + (\mathbf{v} \cdot \nabla - \nabla \cdot \mathbf{D} \cdot \nabla) \bar{M}(u) \bar{P}(\mathbf{x}, u) = 0 \quad (8)$$

for the initial condition $P_0(s) = \delta(s)$, where $\bar{M}(u) = u \bar{\psi}(u) / [1 - \bar{\psi}(u)]$, with $\bar{\psi}(u)$ the Laplace transform of $\psi(\Delta t)$ [34]. The velocity \mathbf{v} and dispersivity \mathbf{D} in (8) are given in terms of $\rho_{\Delta \mathbf{x}}$ as $v_i = \int_{\mathbf{x}} x_i \rho_{\Delta \mathbf{x}}(\mathbf{x}) d\mathbf{x}$, $D_{i,j} = \frac{1}{2} \int_{\mathbf{x}} x_i x_j \rho_{\Delta \mathbf{x}}(\mathbf{x}) d\mathbf{x}$. In the case of longitudinal dispersion, the solution of (8) in the z direction is given in terms of the j th spatial moment of $\bar{P}(z, u)$ as

$$\bar{m}_j(u) = (1+j)! \frac{(a-b) + (-1)^j (a+b)^{-1-j}}{2m_{2,z} \bar{M}(u)^\alpha}, \quad (9)$$

where $a = b\sqrt{1 + u/b^2 \bar{M}(u)}$, $b = \frac{m_{1,z}}{2m_{2,z}}$, and $m_{j,z}$ is the j th moment of $\rho_{\Delta z}$.

For the power-law distribution $\psi(\Delta t)$ (7),

$$\bar{\psi}(u) = 1 - \gamma^* u + u \ln u, \quad (10)$$

with γ^* is Euler's gamma constant. The inverse Laplace transform of the moments \bar{m}_1 and \bar{m}_2 in (9) yields asymptotic expressions for the leading spatial moments of $P(z, t)$ as

$$m_1(t) \approx \frac{m_{1,z} t}{\ln(t)}, \quad (11)$$

$$m_2(t) \approx \frac{m_{1,z}^2 t^2}{\ln(t)^2} + \frac{m_{1,z}^2 t^2}{(\ln(t))^3} + \frac{2m_{2,z} t}{\ln(t)}. \quad (12)$$

Hence, given Poiseuille flow at the pore scale (7), any bounded z increment $\rho_{\Delta z}$ gives longitudinal sublinear mean velocity and superlinear (anomalous) dispersion.

At shorter times, preasymptotic transport cannot be analytically determined from (9), however the simplicity of the model 3D porous network [where $\rho(\Delta z) = \delta(\Delta z - 1)$] allows longitudinal transport to be determined as the sum $t_n = \sum_{i=1}^n \Delta t_i$. While the variance of $\psi(\Delta t)$ is unbounded, the generalized central limit theorem (GLCT) [37] states that the sum of independent and identically distributed random variables (Δt) with unbounded variance converges to a stable distribution $\rho_S(\tau)$ when scaled and shifted (by δ and γ). For $\psi(\Delta t)$, the sum t_n upon scaling and shifting converges to the

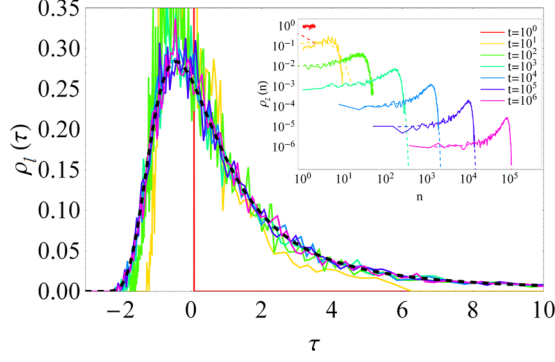


FIG. 3. (Color online) Convergence of the residence time distribution for 10^5 orbits in a single realization of the random network upon shifting and scaling to the Landau distribution $\rho_l(\tau)$. The inset shows a comparison between the analytic (dashed) and the numerical (solid) axial distribution $\rho_L(n)$.

Landau distribution [38]

$$\rho_l(\tau) = \frac{1}{\pi} \int_0^\infty \exp(-\zeta \ln \zeta - \tau \zeta) \sin(\pi \zeta) d\zeta \quad (13)$$

and the shift and scaling variables are $\delta = n\frac{\pi}{2}$ and $\gamma \approx n(\ln n + 1 - \gamma^* - \ln \frac{2}{\pi})$, where n is the number of pore branches and mergers. Hence the preasymptotic residence time distribution (RTD) is well approximated by $\rho_l(\tau)$, as illustrated by convergence of the rescaled RTD from the 3D random network model to $\rho_l(\tau)$ at small n shown in Fig. 3. To quantify pre-asymptotic dispersion in terms of axial dispersion, the RTD $\rho_l(t_n)$ is converted into the axial distribution $\rho_L(n)$ in terms of the pore element number n as

$$\rho_L(n; t) = \left| \frac{\partial \tau}{\partial n} \right| \rho_l(\tau) = \frac{2}{\pi} \left(\frac{1}{n} + \frac{t}{n^2} \right) \rho_l \left(\frac{t - \gamma}{\delta} \right), \quad (14)$$

which agrees well with numerical results from the 3D network model for $t \gtrsim 10$ (Fig. 3). Hence the CTRW (2) and (1) acts as an excellent proxy for ergodic mixing, due to both convergence of the GLCT and decaying correlations arising from the infinite-time Lyapunov exponent λ_∞ . As chaotic advection is inherent to all porous media flow [22], the CTRW model is generally applicable to porous media; although the kernels ψ and $\rho_{\Delta x}$ may differ quantitatively, these results are qualitatively universal.

From (14), preasymptotic longitudinal variance $\sigma_L^2(t)$ is given by the second central moment of ρ_n ,

$$\sigma_L^2(t) = \int_0^{\infty+} [n - \mu_n(t)]^2 \rho_n(n_t) dn, \quad (15)$$

with $\mu_n(t)$ the first moment of ρ_n . Although analytic integration of (15) is not possible, numerical integration of (15) is indistinguishable from numerical simulations of the 3D network model (Fig. 4). Asymptotic longitudinal variance is determined by consideration of the stretching CTRW with (2) replaced by $z_{n+1} = z_n + \Delta z$. From the moments (11) and (12)

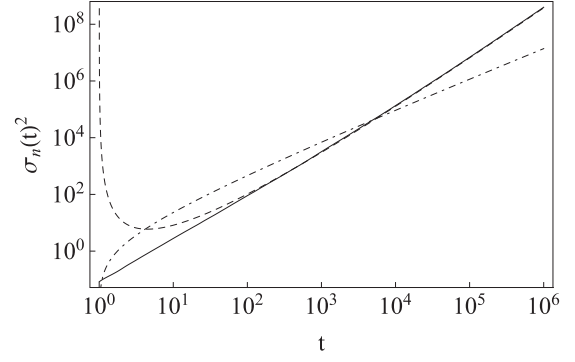


FIG. 4. Longitudinal dispersion $\sigma_L^2(t) \sim \frac{t^2}{(\ln t)^3}$ as predicted by the asymptotic estimate in (16) (dashed line), pore network simulations (solid line), and numerical integration of (15) (solid line). The prediction of axial dispersion in a chaotic duct flows [24] as $\sigma_L^2(t) \sim t \ln(t)$ (dot-dashed line).

the asymptotic longitudinal variance is estimated as

$$\sigma_L^2(t) \sim \frac{t^2}{(\ln t)^3}, \quad (16)$$

which agrees well with both the 3D pore network model and numerical integration of (15) at long times ($t \gtrsim 10^3$) (Fig. 4). Hence the impact of chaotic advection in the 3D model network is to retard longitudinal dispersion from ballistic $\sigma_L^2(t) \sim t^2$ to superdiffusive anomalous transport $\sigma_L^2(t) \sim t^2/(\ln t)^3$.

The pore space geometry and topology of real homogeneous media is more complex than that of the ideal 3D network considered herein, leading to different transverse stretching rates λ_∞ and spatial $\rho_{\Delta z}$ and temporal $\psi(\Delta t)$ increments in the CTRW model. Note that λ_∞ does not directly impact longitudinal dispersion, but only ensures ergodicity of fluid orbits, which renders the CTRW model valid, and so only the spatial and temporal increments control longitudinal dispersion. From (11) and (12), the asymptotic scaling (16) holds for all $\rho_{\Delta z}$ under the Poiseuille time increment (7). In general, longitudinal dispersion for any media can be derived from (9), given $\psi(\Delta t)$ and $\rho_{\Delta z}(\Delta z)$, however the inverse Laplace transform must typically be performed numerically. As the no-slip boundary condition always generates unbounded temporal increments $\psi(\Delta t)$, then from (9), for any spatial increment distribution $\rho_{\Delta z}(\Delta z)$, chaotic advection generates preasymptotic and asymptotic transport, which are universally anomalous (superlinear and sub-ballistic).

The topological complexity inherent to all porous media generates chaotic advection that can significantly augment transport under steady flow conditions. We explore these concepts via an ideal 3D random network model that represents the minimum topological complexity and disordered common to all homogeneous porous media, such that the qualitative features of this model are universal to all porous media. The impact of chaotic Lagrangian dynamics upon nondiffusive transport is profound, with anomalous transport observed for both preasymptotic and asymptotic longitudinal dispersion. These results impact modeling of transport in both heterogeneous and homogeneous porous media and question the validity of the assumption of Fickian transport in homogeneous porous media.

- [1] Z. Warhaft, *Annu. Rev. Fluid Mech.* **32**, 203 (2000).
- [2] A. M. Tartakovsky, D. M. Tartakovsky, and P. Meakin, *Phys. Rev. Lett.* **101**, 044502 (2008).
- [3] B. Berkowitz, A. Cortis, M. Dentz, and H. Scher, *Rev. Geophys.* **44** (2006).
- [4] J. D. Seymour, J. P. Gage, S. L. Codd, and R. Gerlach, *Phys. Rev. Lett.* **93**, 198103 (2004).
- [5] R. Friedrich, J. Peinke, M. Sahimi, and M. R. R. Tabar, *Phys. Rep.* **506**, 87 (2011).
- [6] B. Bijeljic, P. Mostaghimi, and M. J. Blunt, *Phys. Rev. Lett.* **107**, 204502 (2011).
- [7] S. P. Neuman and D. M. Tartakovsky, *Adv. Water Resour.* **32**, 670 (2009).
- [8] T. H. Solomon, E. R. Weeks, and H. L. Swinney, *Phys. Rev. Lett.* **71**, 3975 (1993).
- [9] D. L. Koch and J. F. Brady, *J. Fluid Mech.* **154**, 399 (1985).
- [10] M. G. Trefry, D. R. Lester, G. Metcalfe, A. Ord, and K. Regenauer-Lieb, *J. Contam. Hydrol.* **127**, 15 (2012).
- [11] G. Metcalfe, D. Lester, A. Ord, P. Kulkarni, M. Trefry, B. E. Hobbs, K. Regenauer-Lieb, and J. Morris, *Philos. Trans. R. Soc. London Ser. A* **368**, 217 (2010).
- [12] M. Levy and B. Berkowitz, *J. Contam. Hydrol.* **64**, 203 (2003).
- [13] S. E. Silliman and E. S. Simpson, *Water Resour. Res.* **23**, 1667 (1987).
- [14] E. Major, D. A. Benson, J. Revielle, H. Ibrahim, A. Dean, R. M. Maxwell, E. Poeter, and M. Dogan, *Water Resour. Res.* **47**, W10519 (2011).
- [15] M. Bromly and C. Hinz, *Water Resour. Res.* **40**, W0702 (2004).
- [16] B. Bijeljic, A. H. Muggeridge, and M. J. Blunt, *Water Resour. Res.* **40**, W11501 (2004).
- [17] X. Zhang and M. Lv, *Water Resour. Res.* **43**, W07437 (2007).
- [18] C. P. Lowe and D. Frenkel, *Phys. Rev. Lett.* **77**, 4552 (1996).
- [19] H. Brenner, *Philos. Trans. R. Soc. London Ser. A* **297**, 81 (1980).
- [20] G. Taylor, *Philos. Trans. R. Soc. London Ser. A* **219**, 186 (1953).
- [21] R. Aris, *Philos. Trans. R. Soc. London Ser. A* **235**, 67 (1956).
- [22] D. R. Lester, G. Metcalfe, and M. G. Trefry, *Phys. Rev. Lett.* **111**, 174101 (2013).
- [23] I. Mezić, S. Wiggins, and D. Bantz, *Chaos* **9**, 173 (1999).
- [24] S. W. Jones and W. R. Young, *J. Fluid Mech.* **280**, 149 (1994).
- [25] C. Scholz, F. Wirner, J. Götz, U. Rude, G. E. Schröder-Turk, K. Mecke, and C. Bechinger, *Phys. Rev. Lett.* **109**, 264504 (2012).
- [26] *Morphology of Condensed Matter*, edited by K. Mecke and D. Stoyan, Lecture Notes in Physics, Vol. 600 (Springer, Berlin, 2002).
- [27] R. S. MacKay, *Philos. Trans. R. Soc. London Ser. A* **359**, 1479 (2001).
- [28] J. Slipantschuk, O. F. Bandtlow, and W. Just, *J. Phys. A: Math. Theor.* **46**, 075101 (2013).
- [29] L. A. Bunimovich, *Zh. Eksp. Teor. Fiz.* **89**, 1452 (1985) [*Sov. Phys. JETP* **62**, 842 (1985)].
- [30] D. R. Lester, G. Metcalfe, and M. G. Trefry (unpublished).
- [31] J. M. Ottino and S. Wiggins, *Philos. Trans. R. Soc. London Ser. A* **362**, 923 (2004).
- [32] M. K. Singh, P. D. Anderson, and H. E. H. Meijer, *Macromol. Rapid Commun.* **30**, 362 (2009).
- [33] M. K. Singh, T. G. Kang, P. D. Anderson, H. E. H. Meijer, and A. N. Hrymak, *AIChE J.* **55**, 2208 (2009).
- [34] M. Dentz, A. Cortis, H. Scher, and B. Berkowitz, *Adv. Water Resour.* **27**, 155 (2004).
- [35] J. Klafter and R. Silbey, *Phys. Rev. Lett.* **44**, 55 (1980).
- [36] N. G. V. Kampen, *Stochastic Processes in Physics and Chemistry* (Elsevier, Amsterdam, 1992).
- [37] A. N. Kolmogorov and B. V. Gnedenko, *Limit Distributions for Sums of Independent Random Variables* (Addison-Wesley, Reading, 1968).
- [38] G. Samorodnitsky and M. S. Taqqu, *Stable Non-Gaussian Random Processes: Stochastic Models with Infinite Variance* (Chapman and Hall/CRC, Boca Raton, 2000).